Biosensor *system-on-a-chip* including CMOS-based signal processing circuits and 64 carbon nanotube-based sensors for the detection of a neurotransmitter†

Byung Yang Lee,‡[ab] Sung Min Seo,‡[ac] Dong Joon Lee,[ab] Minbaek Lee,[ab] Joohyung Lee,[ab] Jun-Ho Cheon,[ac] Eunju Cho,[ab] Hyunjoong Lee,[ac] In-Young Chung,[d] Young June Park,*[ac] Suhwan Kim*[ac] and Seunghun Hong*[ab]

Received 17th August 2009, Accepted 30th November 2009
First published as an Advance Article on the web 14th January 2010
DOI: 10.1039/b916975j

We developed a carbon nanotube (CNT)-based biosensor *system-on-a-chip* (SoC) for the detection of a neurotransmitter. Here, 64 CNT-based sensors were integrated with silicon-based signal processing circuits in a single chip, which was made possible by combining several technological breakthroughs such as *efficient signal processing*, *uniform CNT networks*, and *biocompatible functionalization of CNT-based sensors*. The chip was utilized to detect glutamate, a neurotransmitter, where ammonia, a byproduct of the enzymatic reaction of glutamate and glutamate oxidase on CNT-based sensors, modulated the conductance signals to the CNT-based sensors. This is a major technological advancement in the integration of CNT-based sensors with microelectronics, and this chip can be readily integrated with larger scale lab-on-a-chip (LoC) systems for various applications such as LoC systems for neural networks.

Introduction

Nanoscale biosensors based on carbon nanotubes (CNTs)[1,2] and nanowires (NWs)[3,4] have been extensively studied for advanced biomedical applications such as bio-sensing components in lab-on-a-chip (LoC) systems and real-time diagnostics chips implantable in a human body.[5–7] For such applications, it is crucial to integrate CNT/NW-based biosensors reliably with conventional microelectronics, which has been hindered by numerous fundamental limitations such as unpredictable device characteristics of CNT-based sensors[8,9] and fabrication processes incompatible with microelectronics.[10–13] Furthermore, CNT-based sensor surfaces are often functionalized with toxic chemicals,[14,15] which make them incompatible with biosystems. Herein, we developed a CNT-based biosensor system-on-a-chip (SoC) for the detection of neurotransmitters. Importantly, we provide a single-die system-level solution for the integration of CNT-based sensors and CMOS signal-processing chips by combining several features and techniques such as efficient signal processing strategy to reduce circuit complexity, uniform arrays of CNT-based sensors on CMOS signal-processing circuit,[16–18] and substrate functionalization strategy for biocompatible sensors. This is a significant advancement in combining CNT-based sensors with microelectronics, and should be marked as an important milestone for advanced lab-on-a-chip (LoC) applications.

[a]*Nano-Systems Institute, Seoul National University, Seoul, 151-742, Korea*
[b]*Physics and Astronomy, Seoul National University, Seoul, 151-742, Korea. E-mail: seunghun@snu.ac.kr*
[c]*Electrical Engineering, Seoul National University, Seoul, 151-742, Korea. E-mail: ypark@snu.ac.kr; suhwan@snu.ac.kr*
[d]*Electronics and Communications Engineering, Kwangwoon University, Seoul, 139-701, Korea*

† Electronic supplementary information (ESI) available: Supplementary Methods and Fig. S1–S5. See DOI: 10.1039/b916975j

‡ These two authors contributed equally to this work.

Experimental

Materials and methods

The signal processing chip for the biosensor chip was designed and fabricated by using 0.18 μm CMOS foundry service (Dongbu-Anam, Korea). The chip was comprised of three basic layers: CMOS transistor layer, interconnection layers, and pad layers.

For immobilization of enzymes glutamate oxidase and glucose oxidase, the sample was immersed in 1 : 500 (v/v) 3-aminopropyltriethoxysilane (APTES, Sigma, USA) solution in ethanol (J. T. Baker, USA) solution for 5 min, followed by ethanol rinsing and N_2 drying. Afterwards, the sample was treated with 1.25% (v/v) aqueous solution of glutaraldehyde (Junsei, Japan) for ~1 h, followed by rinsing with deionized water and N_2 drying. Then, 20 μl of ~1 mg ml^{-1} glutamate oxidase (Yamasa, Japan) in 10 mM pH 7.4 Phosphate Buffer Saline (PBS, Sigma, USA) was dropped over the aldehyde-terminated CNT junction. The immobilized enzymes glutamate and glucose oxidase were assessed by detecting the hydrogen peroxide released by the enzymatic reaction of the immobilized glutamate and glucose oxidase with their respective target molecules, L-glutamate and β-D-glucose, using spectrophotometric analysis at λ_{max} of 432 nm. For sensing experiments, Keithley 4200 semiconductor characterization system was used to monitor the conductance change of the transducer. A Pt pseudo-reference electrode used for liquid gating, using $Vg = -0.5$ V.

Detailed experimental procedures can be obtained from the ESI material.†

Fabrication of biosensor SoC chip

Fig. 1a shows the preparation process of the CNT-based biosensor SoC chip. The signal processing chip was comprised of a CMOS transistor (TR) layer, interconnection layer, and pad

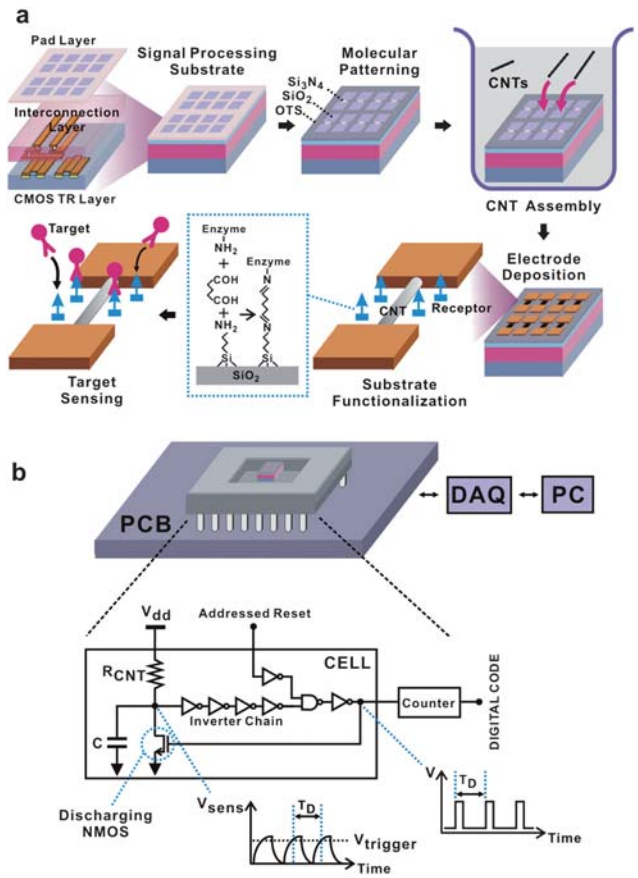

Fig. 1 The fabrication method and signal processing strategy of the CNT-based biosensor SoC. (a) The fabrication process of a CNT-based biosensor SoC. OTS molecular layer was patterned to expose only specific regions of bare Si_3N_4 and SiO_2 surfaces for swCNT adsorption. The molecular patterned chip was dipped into swCNT suspension for CNT assembly. Then, electrodes were formed, and enzymes were immobilized using APTES and glutaraldehyde as linker molecules. (b) A functional diagram showing the signal processing strategy for CNT-based biosensors. The *RC*-charging time of CNT resistors was monitored to measure the signal from CNT-based biosensors. The chipset was wire-bonded to a ceramic package and then mounted on a liquid-immersed PCB. The monitoring was performed with a data acquisition board connected to a PC.

layer. The TR layer incorporated all active devices connected to each other by metal wires of the interconnection layer (Fig. S1†). The pad layer on top of the chip was comprised of source and drain electrode pads (made of Al) obtained by making openings on the final passivation layer (made of SiO_2 and Si_3N_4). On the pad layer, hydrophobic octadecyltrichlorosilane (OTS) self-assembled monolayer (SAM) was patterned *via* photolithography, and the chip was placed in single-walled carbon nanotube (swCNT) solution for 10 s, so that swCNTs were selectively adsorbed onto bare SiO_2 or Al regions without OTS SAM coating.[16–18] Then, Au (30 nm)/Ti (10 nm) electrodes were fabricated *via* a lift-off process. Afterwards, the bare SiO_2 substrate regions below swCNT circuits, instead of swCNT or electrode surfaces,[14,15,19] were functionalized with biomolecules to obtain selective biosensors. Specifically, we coated the SiO_2 surface with 3-aminopropyltriethoxysilane (APTES), and glutamate oxidase was fixed onto the APTES molecules using glutaraldehyde as a linker (Supplementary Information†). Such a "substrate functionalization" strategy allowed us to use well-known biocompatible linking chemistry onto SiO_2 surface, suitable for implantable chips.

Note that the same assembly method can be applied for the integration of CMOS chips with nanowires or carbon electrodes. CNT-based sensors are advantageous for small scale sensor applications. For example, it is still difficult to achieve 'uniform' array of nanowire-based devices. Electrochemical sensors based on carbon electrodes are not suitable for small scale sensor applications because the reduced electrode size results in reduced current signals and poor signal-to-noise ratio. For sensing experiments, the chip was mounted on a printed circuit board (PCB) connected to a data acquisition system (DAQ) controlled by a personal computer (PC) (Fig. 1b). Then, the board was immersed in pH 7.4 PBS buffer, and target molecules were injected while monitoring the conductance.

Results and discussion

Efficient signal processing strategy

In previously-reported sensor experiments, the electric current in CNT sensors was monitored using rather complicated electronics such as pre-amplifiers and ADC circuits. However, such measurement usually required bulky electronics, which are not suitable for high-density biosensor SoC chips. We developed an efficient signal readout circuit for CNT-based sensors (Fig. 1b). Here, the CNT sensor constituted a variable resistor R_{CNT} in a resistor-capacitor (RC) circuit. When the discharging NMOS was switched off, the sensing node voltage V_{sens} charged towards the supply voltage V_{dd}. As V_{sens} reached threshold voltage $V_{trigger}$, the first gate of the inverter chain was activated, and the signal propagated through the chain. The inverter chain introduced appropriate delay to ensure complete charging and discharging of the integrating capacitor C. The signal passed the NAND gate only for the addressed CNT junction, turning the discharging NMOS on. Then V_{sens} went to zero, and the sequence repeated itself. The R_{CNT} change was monitored by measuring the charging-discharging time T_D using counter circuits. Here, *the charging-discharging frequency f was proportional to the conductance G of the swCNT junctions*. The output signals from the counters were multiplexed for all the junctions in the array and passed to the controller.

Uniform array of CNT transducers

Uniform arrays of swCNT transducers were fabricated with a high yield (> 95%) *via the linker-free directed assembly* strategy, where non-polar molecular patterns were utilized to direct the assembly of swCNTs onto specific bare surface regions on the substrate.[16] For example, the assembled CNT transducers in Fig. 2a had a rather uniform resistance distribution in the range of 50 ~ 150 kΩ. Fig. 2b shows detailed adsorption behaviors of swCNTs onto SiO_2. From atomic force microscope (AFM) topography images, we calculated the 'effective thickness' of the adsorbed swCNTs onto SiO_2, which is defined as the volume of adsorbed swCNTs per unit area. We found that if we placed a SiO_2 substrate in swCNT suspensions, after a certain period of

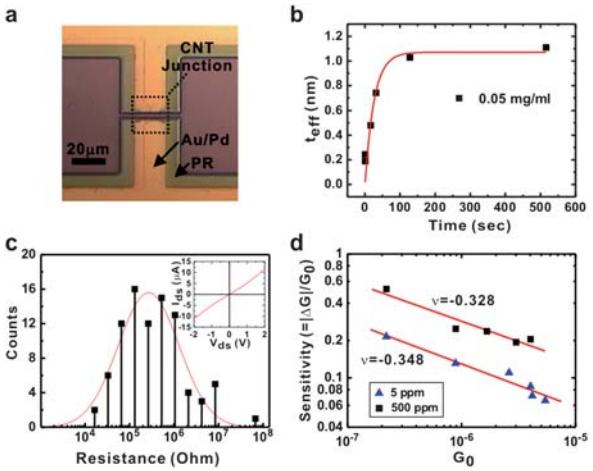

Fig. 2 Uniform array of swCNT-based sensors. (a) Optical micrograph of a polymer-passivated CNT junction. The dashed box points to the exposed CNT junction. (b) Graph showing the effective thickness t_{eff} of adsorbed swCNTs after different dipping time. The amount of adsorbed swCNTs saturated to a terminal value at a given swCNT concentration (0.05 mg ml^{-1}), indicating the *self-limiting* mechanism during the swCNT adsorption process. (c) Resistance distribution of 56 swCNT network junctions. They exhibited a typical *log-normal* distribution of conductive percolating networks. The inset shows a typical IV curve of a CNT network junction. (d) The sensor sensitivity ($|\Delta G|/G_0$) dependence on initial conductance G_0 when exposed to 5 ppm and 500 ppm ammonium hydroxide.

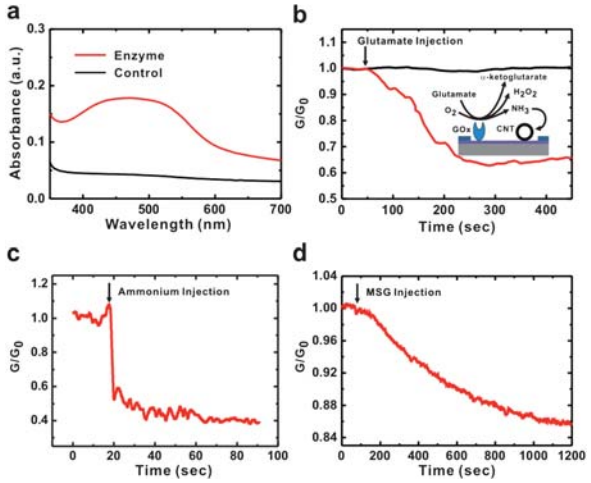

Fig. 3 CNT-based glutamate sensors prepared *via* substrate functionalization. (a) Spectrophotometer signal in the presence (red) and absence (black) of glutamate oxidase immobilized onto the bare substrate between CNT networks. The activity of immobilized GOx was verified by incubating the sample in glutamate solution for 12 h and adding a dye molecule *o*-dianisidine to probe the hydrogen peroxide from the enzymatic reaction. The absorbance spectra from two CNT-based transducers with and without immobilized enzyme clearly imply that our CNT-based transducer is a suitable substrate for biomolecular functionalization. (b) Detection of 100 nM L-glutamate hydrochloride in PBS with (red) and without (black) immobilized glutamate oxidase. The inset shows the detection mechanism where ammonia, one of the by-products, reduced the conductance of swCNTs. (c) Effect of ammonia to the conductance of CNT network-based transducers. The conductance decreased by the injection of 1.4 mM concentration ammonium. (d) Detection of 1mM MSG in PBS using CNT-based glutamate sensors.

time, the amount of adsorbed swCNTs on SiO_2 saturates and converges to a terminal value.[16,20,21] The data could be fitted using the Langmuir-isotherm equation. Presumably, the first adsorbed swCNTs onto bare SiO_2 surface prevent additional adsorptions of swCNTs, resulting in uniform monolayer of swCNT patterns. Such a "self-limiting" mechanism is advantageous in achieving the rather uniform density of CNT networks.[20] The surface density of the adsorbed swCNTs is ~4 μm^{-2}. However, although the channel dimension and density of swCNTs are similar between devices, the final distribution of device conductance shows a large distribution. Fig. 2c shows the conductance distribution of 56 swCNT junctions which were calculated using the slope of the IV characteristic at the linear region around $V_{ds} = 0$. A typical IV curve of a swCNT junction is shown in the inset. The overall distribution can be fitted well by a log-normal distribution. This is a typical behavior of conductive percolating networks.[22,23] Therefore, it is the connectivity of the percolated network channel and not the swCNT density in the channel that determines the sensitivity of the swCNT network junction as a sensor transducer.

Samples with a wide range of initial conductance G_0 were prepared with CNT solutions of different concentrations to study the response $\Delta G/G_0$ of swCNT junctions when exposed to two different concentrations (5 ppm and 500 ppm) of ammonium hydroxide in deionized water (Fig. 2d). Ammonium hydroxide dissolved in water generated ammonium ions which are expected to reduce the conductance of CNT networks.[24] Since ammonium ions were found to play a major role for the detection mechanism of our neurotrasmitter sensors (Fig. 3), the ammonium hydroxide was chosen as a test analyte to study the basic response of our CNT-based sensors. Here, the Au/Pd pads passivated with a photoresist were used as electrodes to minimize the effect of contact resistance and leakage current in liquid environment.[25] The data can be fitted by a function of $|\Delta G|/G_0 \sim G_0^{\nu}$, where ν is a scaling factor. We usually got $0 > \nu > -0.5$. Note that the distribution of sensor response $|\Delta G|/G_0$ was actually narrower than that of the initial conductance G_0 because $|\nu|$ is usually much smaller than 1. CNT junctions with a *higher* initial conductance exhibited *lower* sensor response. Presumably, CNT devices with more metallic swCNTs had higher initial conductance, and therefore lower sensor response. The results indicate that the variation of sensor response should be reduced significantly by using purified semiconducting swCNTs without metallic ones in the future.[26]

Substrate functionalization strategy

Since CNTs were directly adsorbed onto bare substrate regions, bare SiO_2 surface below CNTs can be functionalized by biomolecules to build highly-selective biosensors (Fig. 3). The strategy of functionalizing SiO_2 substrate instead of CNT surfaces[27] can be advantageous because one can utilize well-known biomolecular immobilization chemistry and it can minimize the damage on CNT surfaces. This *substrate functionalization* strategy was tested for various sensor applications such as glutamate, glucose and DNA sensors. In case of glutamate

sensors, glutamate oxidase (GOx) enzymes were immobilized on bare SiO_2 surfaces using APTES and glutaraldehyde as linker molecules (Fig. 3a and Fig. S2†).[28] The activity of immobilized GOx was verified by incubating the sample in glutamate solution for 12 h and adding the dye molecule *o*-dianisidine to probe the production of hydrogen peroxide from the enzymatic reaction (Fig. 3a).[29] The absorbance spectra from two CNT-based transducers with and without immobilized enzymes clearly show that our CNT-based transducer is a suitable substrate for biomolecular functionalization.

For sensor experiments, 40 μl of pH 7.4 PBS was dropped on top of the junction and then 10 μl of target substrate was injected. A constant source–drain bias in the range of 10 mV to 100 mV was applied. A Pt liquid gate electrode was used to reduce noise by keeping the solution at a stable relative potential to the CNTs, while the gate current was monitored to avoid electrochemical reactions.[14,30] Fig. 3b shows the sensor response of CNT junctions with (red) and without (black) immobilized glutamate oxidase when exposed to L-glutamate, a neurotransmitter, indicating selective detection without non-specific response. The enzymatic reaction for glutamate releases several by-products such as hydrogen peroxide, ammonia and α-ketoglutarate. The control experiment revealed that ammonia, one of the by-products, gave sensor signals by reducing the conductance of swCNTs (Fig. 3c).[24,31] The other two by-products, hydrogen peroxide and α-ketoglutarate, showed no effect on the conductance of the CNTs (Fig. S3†). The same glutamate sensor could be used to detect monosodium glutamate (MSG), a food additive related to Chinese food syndrome (Fig. 3d).[32] Also, we used the same strategy to build glucose sensors (Fig. S4†). Glucose oxidase was fixed on bare SiO_2 surface, providing sensor response similar to previous works.[14]

We could also use the same strategy to fabricate DNA sensors. Here, 12 base-pair PNA strands were immobilized onto SiO_2 surfaces (Fig. S5†). Since the PNA molecules had no charge on its backbone, we can expect maximum gating effect onto the swCNT junctions when the charged DNAs bind to the PNA molecules (ESI†). When 22 nM of the non-complementary strand was first injected, we could not observe any change in conductance of the swCNT junction. However, the injection of 13 nM of complementary strand DNA decreased the conductance of swCNT junctions by ~30%. Here, the conductance decrease can be explained by the electron-doping of the negatively-charged hybridizing DNA molecules to the semiconducting CNTs in the channel.[33]

Detection of neurotransmitters with SoC chip

The efficient signal processing strategy (Fig. 1b), uniform array of CNT transducers (Fig. 2), and the substrate functionalization strategy (Fig. 3) were the key breakthroughs which solved the fundamental limitations of previous CNT-based devices and enabled the integration of CNT-based biosensors with CMOS chips (Fig. 4). The biosensor SoC consisted of four independently-functional 8 × 8 array of pixels, a pixel defined as the set of source–drain electrodes and a CNT-based transducer (Fig. 4a). Each pixel was connected to underlying CMOS circuitry to complete the *RC* charge-discharge circuit (Fig. 4b). The address signal ADD designated the specific row and column

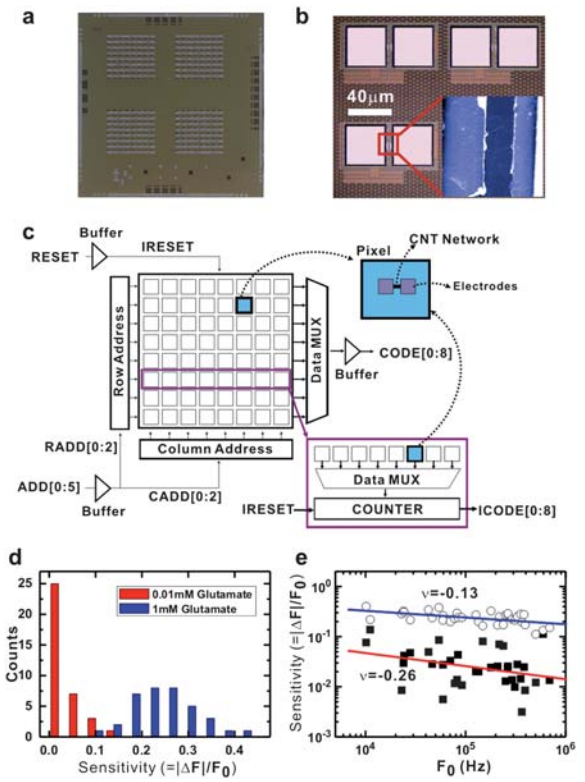

Fig. 4 Operation of a swCNT-based biosensor SoC. (a) Optical micrograph of a biosensor SoC. Each chip (5 mm × 5 mm) has four independently functional 8 × 8 array of CNT network junctions. (b) Magnified optical micrograph showing individual sensors comprised of CNT networks between source and drain electrodes. The inset shows the AFM topography image of swCNT networks between electrodes. (c) Signal flow of the biosensor SoC. (d) Distribution of the sensor sensitivity ($\sim|\Delta f|/f_0$) of the sensors on the SoC chip after the injection of 0.01 mM (red bars) and 1 mM (blue bars) L-glutamate. (e) Graph showing the sensor sensitivity ($\sim|\Delta f|/f_0$) *versus* initial frequency f_0.

address used to select a sensor site for readout (Fig. 4c). The RESET signal enabled the frequency to be read for a fixed signal duration. The counter bits were multiplexed and finally transferred to the DAQ board. 36 junctions out of 64 devices had the conductance values in the range of the signal processing circuits. The other junctions showed too low conductance for detection. For the 36 junctions, the process of enzyme immobilization resulted in little effect in frequency shift, indicating that the *substrate functionalization* scheme is advantageous for retaining the electrical properties of the swCNT junctions during enzyme immobilization.

The conductance was monitored in parallel for the 36 junctions as L-glutamate was injected (Fig. 4d). The conductance G of a swCNT junction is proportional to the measured charge-discharge frequency of f (Fig. 1b). Here, the sensor response can be written as $|\Delta G|/G_0 = |\Delta f|/f_0$. Fig. 4d shows the distribution of the sensor response $|\Delta f|/f_0$ ($=|\Delta G|/G_0$) measured by the biosensor SoC after glutamate injection. The initial sharp distribution around $|\Delta f|/f_0$ ($=|\Delta G|/G_0$) = 0 shifted to higher values and became wider as target concentration increased from 0.01 mM (red bars) to 1 mM (blue bars), due to ammonia adsorption to swCNTs from the enzymatic reactions. Although there was some

variation, the sensors exhibited relatively uniform response to the target molecules. Scaling analysis showed sensor response $|\Delta f|/f_0 \sim f_0^{\nu}$nwith $0 > \nu > -0.5$ (Fig. 4e), which is similar as the conductance variation $|\Delta G|/G_0$ of CNT-based sensors measured using a high-precision preamplifier (Fig. 2b). This result clearly showed that our CNT-based biosensor SoC was functioning properly just like CNT-based sensors equipped with high precision electronics.

Conclusions

In summary, we demonstrated a CNT-based biosensor SoC comprised of 64 swCNT-based biosensors and CMOS-based signal processing circuits in a single chip. Such an implementation was made possible by overcoming several technological hurdles such as the development of *efficient signal processing strategy*, assembly of *uniform CNT devices via* the linker-free directed assembly method, and biocompatible *substrate functionalization* strategy. This result can be an important milestone toward the integration of CNT-based sensors with CMOS chips, and it should open up various biomedical applications such as sensing components in LoC systems for neuronal culture and real-time monitoring devices implantable in a human body.

Acknowledgements

This work was supported by the NANO-Systems Institute National Core Research Center (NSI-NCRC) program. SH acknowledges the partial support from KOSEF grant (No. 2009-0079103), System 2010 program of MKE, and the Conversing Research Center Program of National Research Foundation of Korea (No. 2009-0081999).

Notes and references

1 J. Guo, M. Lundstrom and S. Datta, *Appl. Phys. Lett.*, 2002, **80**, 3192–3194.
2 M. S. Purewal, Y. Zhang and P. Kim, *Phys. Status Solidi B*, 2006, **243**, 3418–3422.
3 Y. W. Heo, L. C. Tien, Y. Kwon, D. P. Norton, S. J. Pearton, B. S. Kang and F. Ren, *Appl. Phys. Lett.*, 2004, **85**, 2274–2276.
4 Z. L. Wang, *J. Mater. Chem.*, 2005, **15**, 1021–1024.
5 M. C. McAlpine, H. Ahmad, D. Wang and J. R. Heath, *Nat. Mater.*, 2007, **6**, 379–384.
6 F. Patolsky, B. P. Timko, G. H. Yu, Y. Fang, A. B. Greytak, G. F. Zheng and C. M. Lieber, *Science*, 2006, **313**, 1100–1104.
7 P. E. Sheehan and L. J. Whitman, *Nano Lett.*, 2005, **5**, 803–807.
8 R. H. Baughman, A. A. Zakhidov and W. A. de Heer, *Science*, 2002, **297**, 787–792.
9 I. Heller, A. M. Janssens, J. Mannik, E. D. Minot, S. G. Lemay and C. Dekker, *Nano Lett.*, 2008, **8**, 591–595.
10 Y. Huang, X. F. Duan, Q. Q. Wei and C. M. Lieber, *Science*, 2001, **291**, 630–633.
11 R. Krupke, F. Hennrich, H. B. Weber, M. M. Kappes and H. von Lohneysen, *Nano Lett.*, 2003, **3**, 1019–1023.
12 S. J. Oh, J. Zhang, Y. Cheng, H. Shimoda and O. Zhou, *Appl. Phys. Lett.*, 2004, **84**, 3738–3740.
13 Y. G. Zhang, A. L. Chang, J. Cao, Q. Wang, W. Kim, Y. M. Li, N. Morris, E. Yenilmez, J. Kong and H. J. Dai, *Appl. Phys. Lett.*, 2001, **79**, 3155–3157.
14 K. Besteman, J. O. Lee, F. G. M. Wiertz, H. A. Heering and C. Dekker, *Nano Lett.*, 2003, **3**, 727–730.
15 R. J. Chen, Y. G. Zhang, D. W. Wang and H. Dai, *J. Am. Chem. Soc.*, 2001, **123**, 3838–3839.
16 M. Lee, J. Im, B. Y. Lee, S. Myung, J. Kang, L. Huang, Y. K. Kwon and S. Hong, *Nat. Nanotechnol.*, 2006, **1**, 66–71.
17 S. Myung, M. Lee, G. T. Kim, J. S. Ha and S. Hong, *Adv. Mater.*, 2005, **17**, 2361–2364.
18 S. G. Rao, L. Huang, W. Setyawan and S. Hong, *Nature*, 2003, **425**, 36–37.
19 X. W. Tang, S. Bansaruntip, N. Nakayama, E. Yenilmez, Y. L. Chang and Q. Wang, *Nano Lett.*, 2006, **6**, 1632–1636.
20 J. Im, L. Huang, J. Kang, M. Lee, D. J. Lee, S. G. Rao, N. K. Lee and S. Hong, *J. Chem. Phys.*, 2006, **124**, 224707.
21 J. Im, J. Kang, M. Lee, B. Kim and S. Hong, *J. Phys. Chem. B*, 2006, **110**, 12839–12842.
22 B. Y. Lee, K. Heo, J. H. Bak, S. U. Cho, S. Moon, Y. D. Park and S. Hong, *Nano Lett.*, 2008, **8**, 4483–4487.
23 R. Rammal, M.-A. Lemieux and A.-M. S. Tremblay, *Phys. Rev. Lett.*, 1985, **54**, 1087.
24 J. Kong, N. R. Franklin, C. W. Zhou, M. G. Chapline, S. Peng, K. J. Cho and H. J. Dai, *Science*, 2000, **287**, 622–625.
25 N. Nemec, D. Tomanek and G. Cuniberti, *Phys. Rev. Lett.*, 2006, **96**, 076802.
26 M. S. Arnold, A. A. Green, J. F. Hulvat, S. I. Stupp and M. C. Hersam, *Nat. Nanotechnol.*, 2006, **1**, 60–65.
27 H.-M. So, K. Won, Y. H. Kim, B.-K. Kim, B. H. Ryu, P. S. Na, H. Kim and J.-O. Lee, *J. Am. Chem. Soc.*, 2005, **127**, 11906–11907.
28 C. D. Stalikas, M. I. Karayannis and S. M. Tzouwarakarayanni, *Analyst*, 1993, **118**, 723–726.
29 N. G. Wilson, T. McCreedy and G. M. Greenway, *Analyst*, 2000, **125**, 237–239.
30 S. Rosenblatt, Y. Yaish, J. Park, J. Gore, V. Sazonova and P. L. McEuen, *Nano Lett.*, 2002, **2**, 869–872.
31 K. Bradley, J. C. P. Gabriel, M. Briman, A. Star and G. Gruner, *Phys. Rev. Lett.*, 2003, **91**, 218301.
32 H. H. Schaumburg, R. Byck, R. Gerstl and J. H. Mashman, *Science*, 1969, **163**, 826–828.
33 A. Star, E. Tu, J. Niemann, J. C. P. Gabriel, C. S. Joiner and C. Valcke, *Proc. Natl. Acad. Sci. U. S. A.*, 2006, **103**, 921–926.

